lubricants

MDPI

Article

Viscosity and Friction Reduction of Double-End-Capped Polyalkylene Glycol Nanolubricants for Eco-Friendly Refrigerant

Mohd Zaki Sharif [1], Wan Hamzah Azmi [1,2,*], Mohd Fairusham Ghazali [1,2], Nurul Nadia Mohd Zawawi [1] and Hafiz Muhammad Ali [3,*]

[1] Centre for Research in Advanced Fluid and Processes, Lebuhraya Tun Razak, Kuantan 26300, Pahang, Malaysia
[2] Faculty of Mechanical and Automotive Engineering Technology, Universiti Malaysia Pahang, Pekan 26600, Pahang, Malaysia
[3] Mechanical Engineering Department, King Fahd University of Petroleum and Minerals, Dhahran 31261, Saudi Arabia
* Correspondence: wanazmi@ump.edu.my (W.H.A.); hafiz.ali@kfupm.edu.sa (H.M.A.)

Abstract: In sustainable tribology, researchers are investigating methods to enhance tribological performance by incorporating nanoparticles into lubricants. However, one potential drawback of this strategy is increased lubricant viscosity. The current study aimed to assess the impact of these nanoparticles on the viscosity and coefficient of friction (COF) of the nanolubricants. Three different nanolubricants were synthesized through a two-step process, including mono-nanolubricants (Al_2O_3/DEC PAG and SiO_2/DEC PAG) and hybrid nanolubricants (Al_2O_3-SiO_2/DEC PAG), at volume concentrations between 0.01% and 0.05%. The viscosity and shear flow behavior of these nanolubricants were evaluated using a digital rheometer, while the COF was measured using a Koehler four-ball tribometer. All the nanolubricants showed Newtonian behavior during the experiments. The dynamic viscosity velocity increment of SiO_2/DEC PAG was found to be the lowest (1.88%), followed by Al_2O_3-SiO_2/DEC PAG (2.74%) and Al_2O_3/DEC PAG (3.56%). The viscosity indices of all the nanolubricants were improved only at higher concentrations. At a volume concentration of 0.03%, the Al_2O_3-SiO_2/DEC PAG nanolubricant reduced the COF by up to 8.1%. The results showed that the combination of nanoparticles, temperature, and volume concentration significantly influenced the viscosity and COF of nanolubricants. This study provides essential information for developing high-performance nanolubricants with improved viscosity and COF and advancing environmentally friendly tribology solutions.

Keywords: nanolubricants; viscosity; friction reduction; double-end-capped PAG; refrigeration system

Citation: Sharif, M.Z.; Azmi, W.H.; Ghazali, M.F.; Zawawi, N.N.M.; Ali, H.M. Viscosity and Friction Reduction of Double-End-Capped Polyalkylene Glycol Nanolubricants for Eco-Friendly Refrigerant. *Lubricants* **2023**, *11*, 129. https://doi.org/10.3390/lubricants11030129

Received: 10 February 2023
Revised: 6 March 2023
Accepted: 8 March 2023
Published: 12 March 2023

1. Introduction

In the context of the current global concerns about global warming, stricter pollution regulations, and a push towards more energy-efficient vehicles, there is a need to improve the efficiency of automotive air-conditioning (AAC) systems. A critical aspect of AAC systems is the compressor-lubricating fluid used. Polyalkylene glycol (PAG) is commonly utilized for its ease of use, availability, and low cost [1,2]. Green tribology emphasizes the aspects of interacting surfaces in relative motion that are important for energy or environmental sustainability, including tribological technology that mimics living nature. The use of alternative refrigerants such as R1234yf is acceptable for new passenger cars and light-duty trucks due to its low global warming potential (GWP) of 1 [3]. However, when using the refrigerant R1234yf, which has a high moisture content, it is necessary to use a lubricant that does not absorb moisture to prevent harm to the compressor from the reaction between the lubricant and moisture. To address this issue, double-end-capped

polyalkylene glycol (DEC PAG) is used in AAC-R1234yf systems. However, compared to the AAC-R134a system, the performance of the AAC-R1234yf system is lower [4]. Therefore, it is essential to improve the tribology and thermophysical properties of DEC PAG. One approach to achieving this is adding nanoparticles as additives [5]. Adding metal oxide nanoparticles is expected to improve the thermophysical characteristics of DEC PAG due to the higher thermal conductivity of metals compared to liquids [6].

In green tribology, proper lubrication of compressors is crucial in reducing friction and preserving the wall's surface [7]. The incorporation of nanoparticles into the lubricant can result in a significant increase in viscosity. This situation must be taken into account when considering the use of nanoparticles in lubricants. Studies have shown that different types of nanoparticles have unique effects on viscosity. For example, Ma et al. [8] found that the viscosity of nanolubricants can increase by as much as 23.5%. Haldar et al. [9] observed that as the concentration of MWCNT/SiO_2 nanolubricants in hydraulic oil increases, so does its viscosity, particularly at lower temperatures. Similarly, Kedzierski et al. [10] discovered that Al_2O_3/POE and ZnO/POE nanolubricants had 250% and 170% viscosity increases, respectively, when compared to other nanoparticle types. Hybrid nanolubricants can be used to mitigate the impact of increased viscosity [11]. Zawawi et al. [12] compared the performance of hybrid nanolubricants (Al_2O_3-SiO_2, Al_2O_3-TiO_2, and TiO_2-SiO_2) dispersed in PAG lubricants to that of single-particle nanolubricants. The results showed that hybrid nanolubricants had smaller increases in viscosity and superior thermal conductivity compared to single-particle nanolubricants. This research suggests that hybrid nanolubricants may be more suitable for refrigeration systems, but carefully selecting the nanoparticles is essential.

The viscosity of a lubricant can significantly impact its tribological properties. Higher viscosity often results in higher coefficients of friction (COF) [13,14]. However, adding nanoparticles to a lubricant can improve its performance by reducing friction and enhancing the "nano-rolling effect." In liquid lubrication systems, friction and wear rely on the contact surface conditions and the applied load [15]. This demonstrates the need to develop a nanolubricant with low viscosity increment and excellent thermal conductivity enhancement. The tribological properties of a nanolubricant, including the shear flow curve and coefficient of friction, can be influenced by various factors, such as the type, size, shape, concentration, and operating temperature of the nanoparticles used. Research has shown that graphene-based nanolubricants exhibit superior tribological performance to conventional lubricants [16]. Additionally, metal oxide nanoparticles have been found to reduce friction between sliding surfaces, but their abrasiveness may also increase surface wear. Further investigation revealed that ZnO/H_2O and Al_2O_3/H_2O reduced the friction to 56.9% and 53%, respectively [17]. Careful selection of the appropriate nanoparticles is necessary to achieve a nanolubricant with low viscosity increment and enhanced thermal conductivity.

Zawawi et al. [7] studied the COF and wear-rate characteristics of PAG compressor lubricants with composite nanoparticles. Different concentrations of composite nanolubricants were tested using a piston ring tribology test. At 0.02% volume concentration of composite nanolubricants, the COF was reduced to 4.49% and the wear rates were reduced to 12.99%. The study showed that combining composite nanoparticles has high potential for tribology improvement in the refrigeration system. Jeng et al. [18] studied the friction characteristics and wear behavior of carbon nanocapsules (CNCs) in mineral oil lubricants. Tribological analysis was undertaken using block-on-ring tests. The tribological properties of CNC nanolubricants are strongly dependent on the structure variation of the nanoparticles hence verifying the lubrication mechanism of CNCs at the sliding system. In another paper, Jeng et al. [19] examined the tribological performance of carbon–Fe nanocapsule (CFNC) nanolubricants for high-contact loads. They concluded that the CFNC nanolubricants improved the micro-bearing lubrication mechanism, surface permeability, and filling properties. Earlier, Rapoport et al. [20] investigated the potential of hollow nanoparticles (HNs) of MX_2 as solid-state lubricants. The HN-MX_2 performed effectively in friction, wear, and lifetime, allowing the particles to roll rather than slide.

The impact of nanoparticles on the shear curve, viscosity, and coefficient of friction (COF) of a DEC PAG-based nanolubricant has not been thoroughly studied. This study sought to explore the influence of nanoparticles on a nanolubricant based on DEC PAG. Additionally, it is essential to examine the differences in viscosity and COF between mono-nanolubricants (Al_2O_3/DEC PAG and SiO_2/DEC PAG) and hybrid nanolubricants (Al_2O_3-SiO_2/DEC PAG). In this research, nanoparticles of Al_2O_3 and SiO_2 were incorporated into the lubricant using a two-step preparation process. All nanolubricants were prepared with a volume concentration ranging from 0.01% to 0.05%. After the addition of nanoparticles, the shear curve was used to evaluate the Newtonian behavior of the material. Subsequently, the viscosity improvement was compared among all types of nanolubricants. Finally, tribological testing was conducted to assess the impact of nanoparticles on the COF of the newly developed DEC PAG-based nanolubricant.

2. Materials and Methods

2.1. The Materials Specification

Researchers have been interested in metal oxide nanoparticles due to their potential applications in various fields, such as information storage, nanosensors, nanoelectronics, nanodevices, and optoelectronics [21]. These metal oxides are considered more stable due to their oxide bonds. This study used aluminum oxide (Al_2O_3) and silicon dioxide (SiO_2) nanoparticles as nanoadditives, obtained from Sigma-Aldrich in the Missouri, USA and Beijing DK nanotechnology Co., Ltd. in Beijing, China. The manufacturers described the nanoparticles' physical properties, which are presented in Tables 1 and 2. No surfactants were used during the experiments to preserve the integrity of the nanosuspension. Despite the absence of surfactants, the nanolubricants produced in this study were sufficiently stable. The primary lubricant used for the investigation was PAG ND12, which DENSO supplied. PAG ND12 is a low-hygroscopicity DEC PAG lubricant appropriate for use with R1234yf, a refrigerant particularly sensitive to lubricant and moisture interaction.

Table 1. Physical properties of nanoadditives [22,23].

Properties	Al_2O_3	SiO_2
Color	White	White
Purity (%)	99.9	99.9
Density (g/cm^3)	4	2.22
Structure	Spherical	Spherical
Average size (nm)	13	30
Molecular mass, g·mol^{-1}	101.96	60.08
Specific heat, J·(kg·K)$^{-1}$	773	745
Thermal conductivity, W·(m·K)$^{-1}$	36	1.4

Table 2. Chemical and physical properties of the double-end-capped PAG ND12 lubricant [24].

n	Properties	Value
1	ISO viscosity grade	46
2	Dynamic viscosity at 40 °C (mPa·s)	40.13
3	Dynamic viscosity at 100 °C (mPa·s)	8.25
4	Viscosity index	216
5	Density at 15 °C (g/cm^3)	0.988
6	Flash point (°C)	−45

2.2. Nanolubricant Preparation and Stability

This study aimed to investigate the properties of nanolubricants by measuring their shear curve, viscosity, and coefficient of friction with different volume concentrations. The nanolubricants were prepared using a two-step method ideal for incorporating powder

nanoparticles into the base fluid [25]. The required nanoparticle mass was calculated using a 4-digit balance, and the necessary calculations were performed using Equations (1) and (2). In these equations, ϕ, V, m, and ρ represent the volume concentration (%), volume (mL), mass (g), and density (g/cm^3), respectively. The mixture of nanoparticles and the DEC PAG lubricant was stirred for 30 min at 800 to 900 RPM. A Fisherbrand FB11201 advanced ultrasonic bath was used at 60% amplitude for 120 min to enhance the stability of the dispersion. During ultrasonication, the sample temperature reached 75 °C, which is expected to improve dispersion due to decreased base lubricant viscosity at higher temperatures [26].

The size and dispersion conditions of the nanoparticles were measured using transmission electron microscopy (TEM) JSM 7800F. The analysis of the cross-section area for each nanoparticle on the TEM image was determined using ImageJ software to evaluate the average diameter of the particle [5]. Figure 1 presents TEM images of the nanoparticles suspended in the lubricant. The TEM images for nanolubricants with nanoparticles (Al_2O_3, SiO_2, and Al_2O_3-SiO_2) are shown also. From the ImageJ analysis, the average diameter for Al_2O_3 and SiO_2 nanoparticles was ±13 and ±30 nm, respectively. The sizes were confirmed in agreement and consistent with the data provided by the manufacturer. Both nanoparticles were observed in a spherical shape. In addition, the dispersion state for Al_2O_3 and SiO_2 nanoparticles in PAG lubricants was also found in good condition with minimal agglomeration, as shown in Figure 1. However, further quantitative evaluation of stability is required to confirm the actual dispersion conditions of the present nanolubricants using zeta potential and UV-vis measurements.

$$\varphi = \left(\frac{V_p}{V_p + V_{PAG}} \right) \times 100\% \text{ where } m_p = V_p \rho_p \tag{1}$$

$$\varphi = \left(\frac{m_p}{\frac{m_p}{\rho_p} + \frac{m_{PAG}}{\rho_{PAG}}} \right) \times 100\% \tag{2}$$

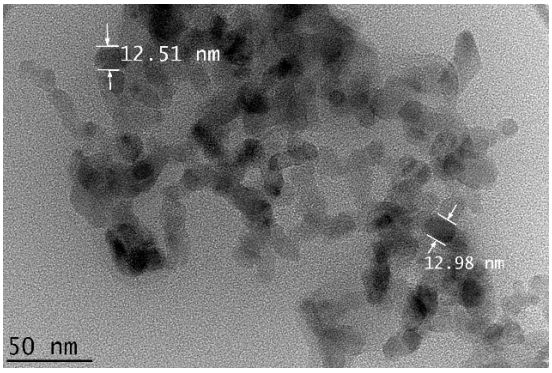

(**a**) Al_2O_3/PAG nanolubricants

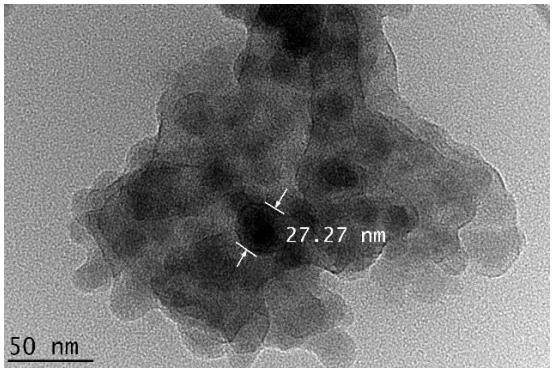

(**b**) SiO_2/PAG nanolubricants

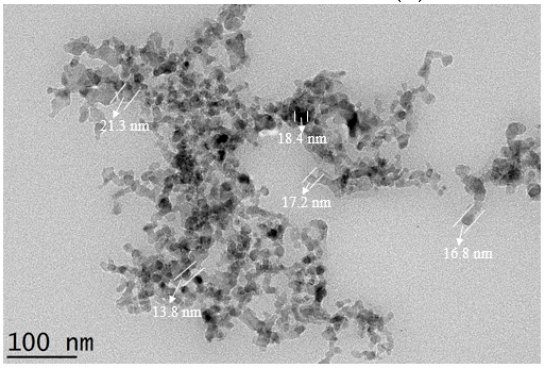

(**c**) Al_2O_3-SiO_2/PAG nanolubricants

Figure 1. TEM images of nanolubricants at different magnifications.

Nanolubricants are considered unstable fluids due to their solid–liquid interactions. Time and temperature during storage and operation can significantly influence their physical characteristics, chemical properties, and stability. The difference in density between the nanoparticles and the lubricant contributes to the stability of the nanolubricants [27]. Over time, nanoparticles will agglomerate and form larger clusters with variable relative densities. These clusters will sink and settle due to gravity when they have a higher density than the lubricant.

The stability of DEC PAG-based nanolubricants was evaluated using zeta potential and UV-vis measurements. The zeta potential provides information about the charge on the nanosurface emulsion. It is often used as an indicator of stability, with a zeta potential more significant than 60 mV indicating excellent stability [28]. The zeta potential was measured using an Anton Paar zeta potential analyzer (Litesizer 500), and the UV-vis measurements were taken using a UV-vis spectrophotometer (Genesys 50).

2.3. Shear Flow Curve and Viscosity Study

In this study, the kinematic viscosity and shear flow curve of nanolubricants were measured at 10 °C increments from 0 °C to 100 °C using a rotating rheometer. The measurements were performed using Anton Paar viscometers (RheolabQC), which have a range of 1 to 109 mPa·s. The double-gap measurement method was employed to evaluate the viscosity of the nanosuspension. The RheolabQC has a servo motor and a high-resolution digital encoder, improving measurement accuracy, especially for low viscosity at low speeds. The encoder records the rotational speed of the measuring bob, and the motor torque sensor measures the viscous drag created in the opposite direction of the measuring bob. The motor current, which is proportional to the torque, is used to calculate the sample's viscosity.

During the verification process, distilled water was used, and each shear flow curve test was performed using a new sample. The sample was allowed to settle for five minutes before the test to ensure a more precise temperature readout. A regression model for the dynamic viscosity of nanolubricants was developed using the average results of the tests. The viscosity index was calculated according to ASTM D2270 and ISO 2909, and it indicates how well the lubricant maintains its viscosity and lubrication across a temperature range. The viscosity index is a unitless value, and it is an essential factor in determining the lubricant's performance.

2.4. Tribology Study

In this study, the tribological performance of nanolubricants was measured using the Koehler four-ball tribotester. The conditions for the tribology testing are summarized in Table 3 and were conducted following the ASTM D4172 standard. The experiment was performed at a speed of 1200 ± 60 rpm with a load of 40.0 ± 0.2 kg for 60 min. An automatic temperature controller was used to regulate and maintain the operating temperature at 75 °C to keep the lubricants at a constant temperature. The test balls used were chromium steel grade G20 balls with a diameter of 12.7 mm and a Rockwell C hardness of 60 ± 1. New steel balls were used for each test. The testing began with pure lubricant and progressed to nanolubricants with different concentrations and component ratios. The friction torque was recorded for both the pure lubricant and the nanolubricants, and the coefficient of friction (COF) was calculated using Equation (3) for each experimental condition. The COF is a measure of the friction between two surfaces, and it was calculated by dividing the friction torque by the normal load. The friction torque, Nm^{-1}, is equal to the normal load, kg, multiplied by the friction coefficient:

$$\mu = 2.23004 \frac{\tau}{F_N} \quad (3)$$

Table 3. Chemical and physical properties of the double-end-capped PAG ND12 lubricant [24].

Standard	Test Conditions			
	Speed (rpm)	Standard	Speed (rpm)	Standard
ASTM D4172 Wear characteristic Test	1200 ± 60	40.0 ± 0.2	60 ± 1	75 ± 2

2.5. Apparatus Reliability Analysis

The Anton Paar viscometers were precalibrated [29] at the manufacturer's factory according to ISO 17025. Before measuring the test fluids, the experimental data were compared to the reference fluid to check the accuracy of both apparatuses. The reference fluid for this purpose was viscosity standard fluid N10 supplied by Anton Paar, which gives 280 mPa·s at 20 °C. The standard fluid at 20 °C was measured to be 281.1 mPa·s, which is only a 1.1 mPa·s difference from the standard value, confirming that the instrument was functioning correctly. The zeta potential analyzer, UV-vis, and rotating viscometer data were collected individually. The fractional uncertainty formula was used to compute the expanded uncertainties for all measured parameters in the current investigation. Table 4 summarizes the uncertainties for the zeta potential, UV-vis, viscosity, nanoparticle concentration, and all other measurements.

Table 4. Summary of fractional uncertainty analysis.

Parameters	Range of Instrument	Values Measured		Lease Division in Instrument	Fractional Uncertainty (%)	
		Min	Max		Min	Max
Nanoparticle weight [g]	0 to 200	0.005	0.1001	±0.0001	0.1	2
Lubricant volume [mL]	1 to 50	100	100	±1	2	2
Volume concentration [%]	-	0.01	0.05	-	1.41	1.68
Zeta potential [mV]	0 to 1000	80.4	140	±0.1	0.07	0.12
Absorbance (UV-vis)	0 to 3	0.011	3	±0.001	0.03	9.1
Shear rate, ε [s^{-1}]	0.01 to 4000	2.15	1070	±0.01	≈0	0.47

3. Results and Discussion

3.1. Stability

The zeta potential analysis was done before the UV-vis and visual sedimentation observation. The Al_2O_3/DEC PAG, SiO_2/DEC PAG, and Al_2O_3-SiO_2/DEC PAG nanolubricants showed zeta potential values of 80.4 mV, 82.6 mV, and 140 mV, respectively, indicating excellent stability. A high zeta potential describes a strong electrokinetic potential layer between nanoparticles, thus preventing agglomeration. Based on the visual observation, no deposition was visible for any nanolubricant. As depicted in Figure 2, the concentration ratio of all three nanolubricant samples decreases at a specific level over six months at a slow pace. The concentration ratio decreases in the first 100 days because particles continue to agglomerate, although at a low pace. Compared to the initial concentration, the Al_2O_3-SiO_2/DEC PAG sample can sustain an average concentration ratio of 0.77, followed by Al_2O_3/DEC PAG and SiO_2/DEC PAG at 0.49 and 0.29, respectively. Throughout the test, the Al_2O_3-SiO_2/DEC PAG and Al_2O_3/DEC PAG samples demonstrate a minimal change of concentration ratio, indicating good stability. However, when the sample reaches 100 days, the agglomeration rate is low and more stable. This condition is due to the strong repulsion between particles, as shown by the zeta potential value, which causes the density difference between the nanoparticle clusters and the DEC PAG lubricant to be insignificant.

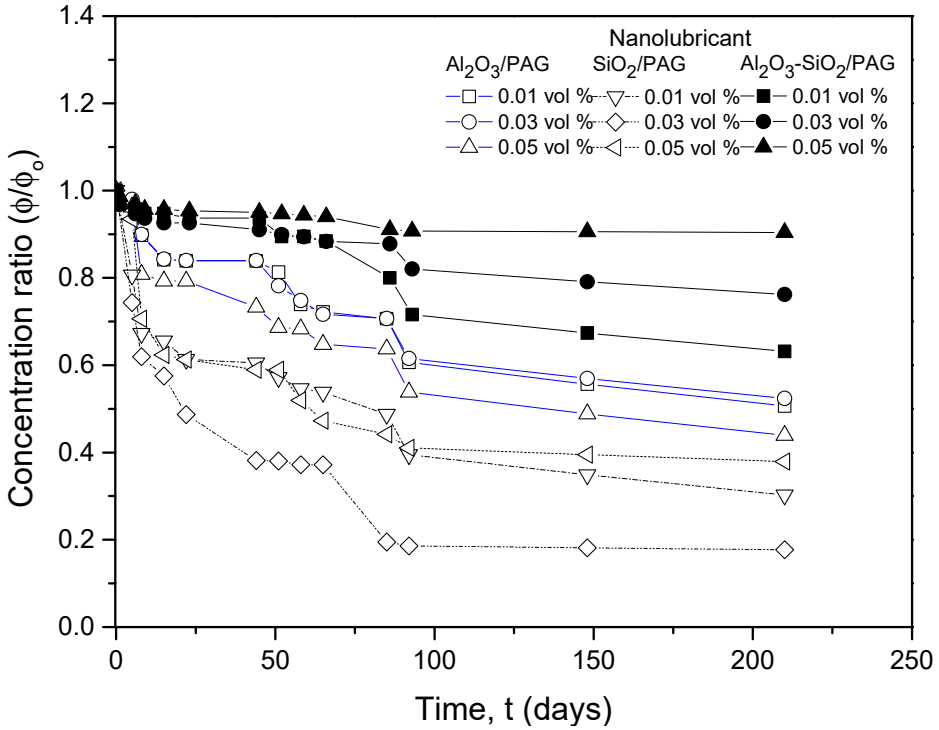

Figure 2. Concentration ratio of nanolubricants with sedimentation time.

3.2. Shear Curve

Figure 3 shows the viscosity of the nanolubricants at different shear rates from 0 to 900 s^{-1} for temperature variations up to 100 °C. The figure presents the dynamic viscosity variation with the shear rate at 0.05% volume concentration for the DEC PAG base lubricants, Al_2O_3/DEC PAG, SiO_2/DEC PAG, and Al_2O_3-SiO_2/DEC PAG nanolubricants. All nanolubricants in the present study behaved as Newtonian fluids. The general characteristics of Newtonian fluids are described as fluids with viscosity independent against shear stress changes. They exhibited Newtonian behavior at high shear rates (higher than 50 s^{-1}) and above. At low shear rates (0 to 50 s^{-1}), the nanolubricants displayed shear thickening characteristics (increased viscosity with increasing shear rate). This behavior is typical of most lubricants. Lubricants are often more viscous than water to keep an active layer of film on the surface of the compressor, hence minimizing friction between the moving surfaces. The shear-thickening phenomenon at lower speeds may change particle orientation and lead to agglomeration integration. If aggregates are present, nanoparticles and lubricant molecules tend to establish a tighter link, increasing the apparent viscosity of nanolubricants. The AAC system is controlled by a thermostat or pressure sensors, and frequent compressor startups will occur. However, suitable lubricants should have only modest shear thickening capabilities to allow the compressor to run with less power during the early rotation cycles. According to the standard in Table 2, the dynamic viscosity for PAG ND12 lubricants at 40 and 100 °C was 40.13 and 8.25 mPa.s, respectively. Meanwhile, the dynamic viscosity of nanolubricants at 40 and 100 °C was measured in the range of 39.63 to 40.83 and 8.55 to 9.10, respectively. Therefore, the dynamic viscosity variation for nanolubricants is within the acceptable range for application in a compressor of AAC-R1234yf systems.

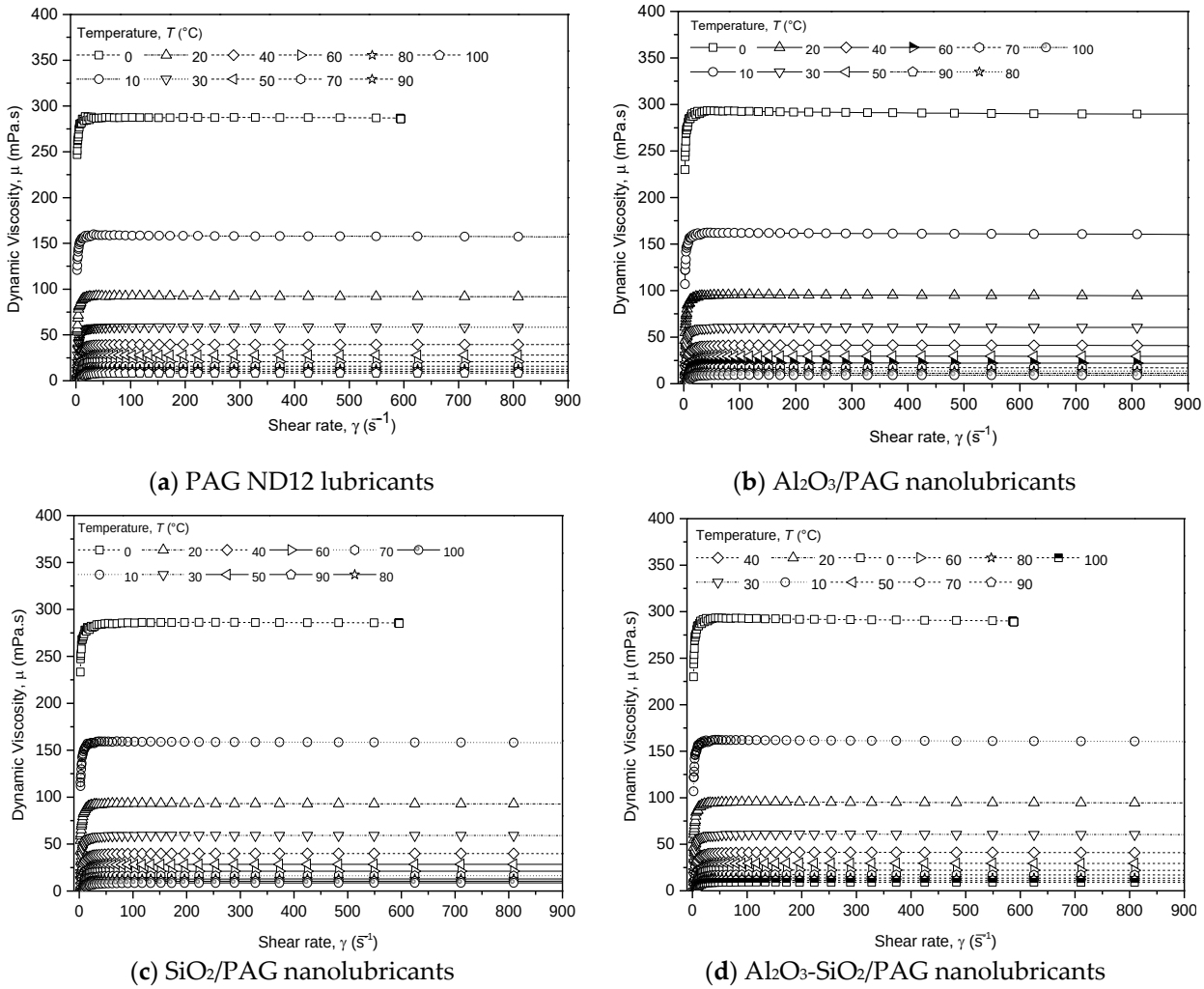

Figure 3. Dynamic viscosity and shear strain rate characteristics of PAG and nanolubricants at 0.05% volume concentration.

Figure 4 presents the shear curves of PAG base lubricants, Al_2O_3/DEC PAG, SiO_2/DEC PAG and Al_2O_3-SiO_2/DEC PAG nanolubricants at a temperature of 0 to 100 °C. The figure shows the shear stress properties with linear relation against shear rate. The linear trends apply for DEC PAG base lubricant and all nanolubricants. Figure 4 shows no shear thickening since shear stress rose proportionately to the shear rate. In other words, the viscosity of nanolubricants remains unchanged no matter how much force is applied to flow through the pipe or channel. In addition, the slope of the graph in the figure represents the viscosity of nanolubricants, and it strongly depends on the temperature. At low temperatures, the slopes are considerably high to denote the high viscosity of fluids and vice versa for high temperatures. Figures 3 and 4 show that the Al_2O_3/DEC PAG, SiO_2/DEC PAG, and Al_2O_3-SiO_2/DEC PAG nanolubricants retain the Newtonian properties for temperatures from 0 to 100 °C and follow the behavior of the original DEC PAG base lubricants. No significant changes in the trend lines and slopes were observed in the graphs when dispersing with different types of nanoparticles into PAG lubricants.

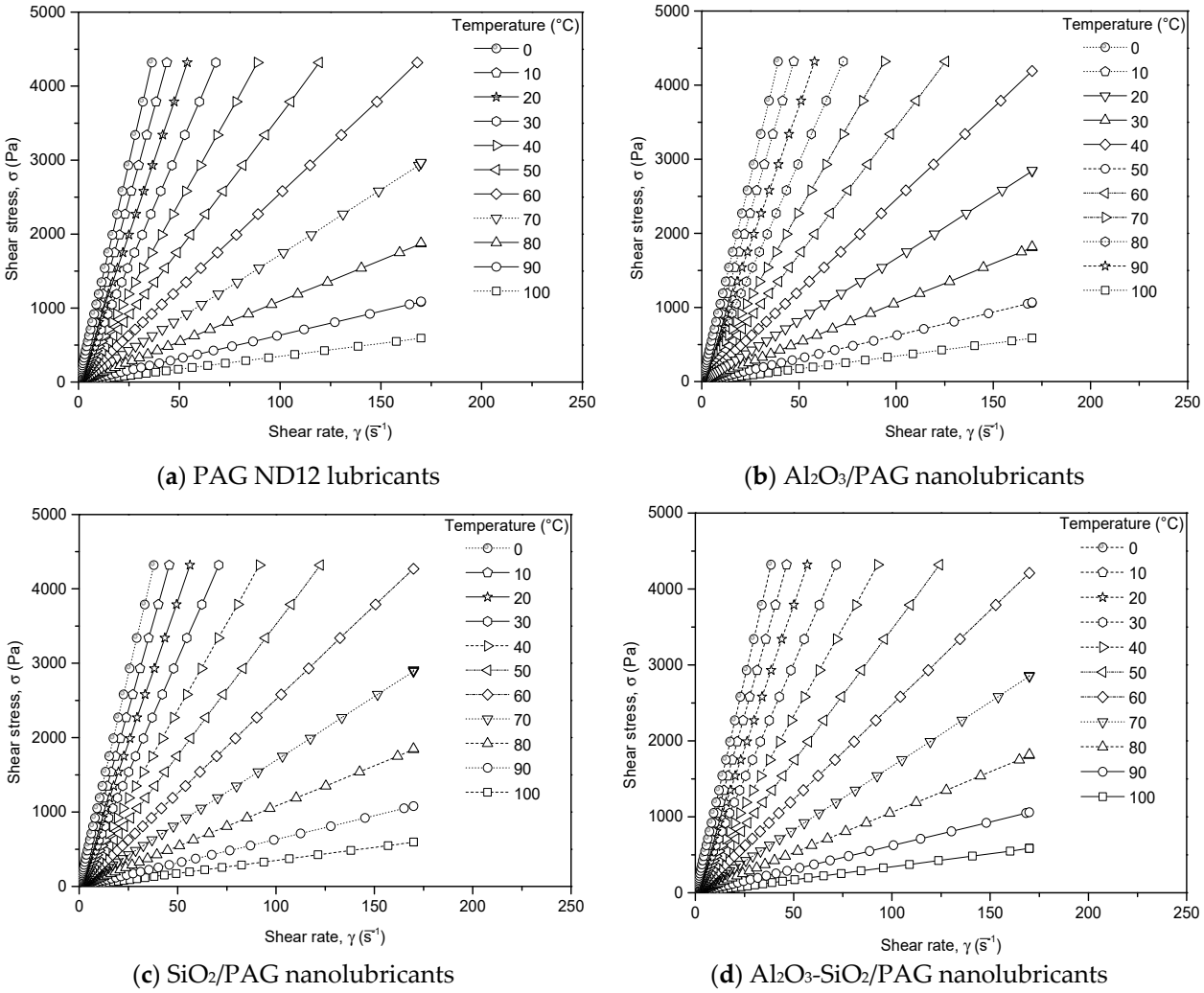

(**a**) PAG ND12 lubricants (**b**) Al_2O_3/PAG nanolubricants

(**c**) SiO_2/PAG nanolubricants (**d**) Al_2O_3-SiO_2/PAG nanolubricants

Figure 4. Shear stress and shear strain rate characteristic of PAG and nanolubricants at 0.05% volume concentration.

3.3. Dynamic Viscosity Evaluation

The dynamic viscosity variation for Al_2O_3/DEC PAG, SiO_2/DEC PAG and Al_2O_3-SiO_2/DEC PAG nanolubricants at various temperatures is shown in Table 5. The viscosity in the figures decreased with increasing temperatures. Similar trends apply to all types of nanolubricants. This is due to the weak intermolecular attraction between DEC PAG molecules and nanoparticles at higher operating temperatures [30]. Temperature increases lead to decreased flow resistance between molecules and rotating measuring cups, which causes viscosity to decrease. The current findings align with those of earlier studies in the literature [31,32]. The viscosity also increased as the volume concentration of nanolubricants rose. This trend is caused by increased flow resistance brought on by the concentration of nanoparticles in nanolubricants.

Figure 5 shows the relative viscosity enhancement for the nanolubricants at various volume concentrations and temperatures. The dynamic viscosity enhancement was increased with volume concentration and applied to all nanolubricants. The results also revealed that the increment in the viscosity for Al_2O_3/DEC PAG nanolubricants was more dominant than for SiO_2/DEC PAG nanolubricants and occurred for all volume concentrations and temperatures. The Al_2O_3/DEC PAG nanolubricants were increased by an average viscosity of up to 3.56% higher than the SiO_2/DEC PAG nanolubricants, with an average increment of 1.88%. It has been demonstrated that the type of nanoparticles and their combination significantly impact the dynamic viscosity of the nanolubricants [12,33].

The Al_2O_3 nanoparticles are characterized by a higher density than SiO_2 nanoparticles, despite their smaller particles, justifying the finding. Consequently, Al_2O_3/DEC PAG nanolubricants contain more nanoparticles for a similar volume concentration, resulting in a higher viscosity increment than SiO_2/DEC PAG nanolubricants.

Table 5. Dynamic viscosity of Al_2O_3/PAG, SiO_2/PAG and Al_2O_3-SiO_2/PAG nanolubricants at different volume concentrations.

Temperature (°C)	Al_2O_3/PAG	SiO_2/PAG	Al_2O_3-SiO_2/PAG	Al_2O_3/PAG	SiO_2/PAG	Al_2O_3-SiO_2/PAG	Al_2O_3/PAG	SiO_2/PAG	Al_2O_3-SiO_2/PAG
	Vol (%)								
	0.01			0.03			0.05		
0	286.37	283.86	286.37	288.67	285.47	288.94	290.54	285.58	291.66
10	158.06	157.14	158.06	160.13	158.10	159.48	160.43	157.95	160.96
20	92.58	92.33	92.58	93.90	92.51	93.59	94.31	92.58	94.40
30	58.81	58.87	58.81	59.84	58.79	59.42	60.24	58.99	60.04
40	39.70	39.63	39.70	40.45	39.72	40.16	40.83	39.84	40.54
50	28.31	28.21	28.31	28.84	28.32	28.61	29.20	28.40	28.91
60	21.22	20.97	21.22	21.50	21.11	21.28	21.83	21.16	21.52
70	16.35	16.14	16.35	16.57	16.33	16.39	16.90	16.38	16.60
80	12.73	12.78	12.73	13.17	12.99	12.98	13.46	13.00	13.18
90	10.40	10.36	10.40	10.71	10.56	10.53	10.97	10.57	10.73
100	8.70	8.55	8.70	8.89	8.74	8.67	9.10	8.77	8.89

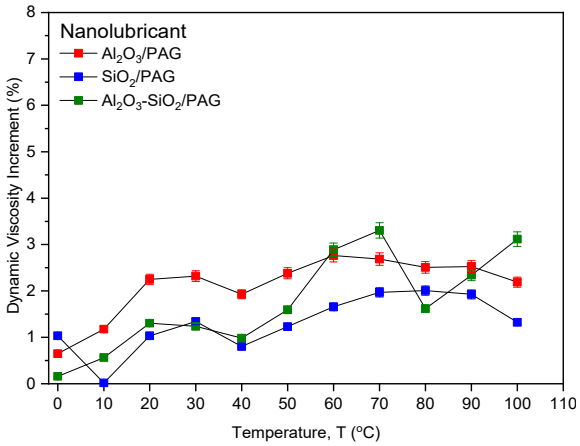

(**a**) 0.01% volume concentration

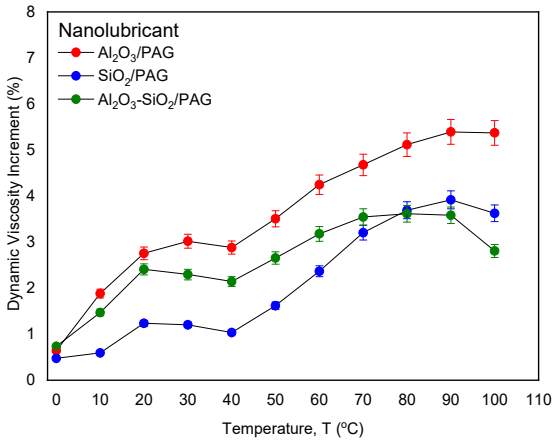

(**b**) 0.03% volume concentration

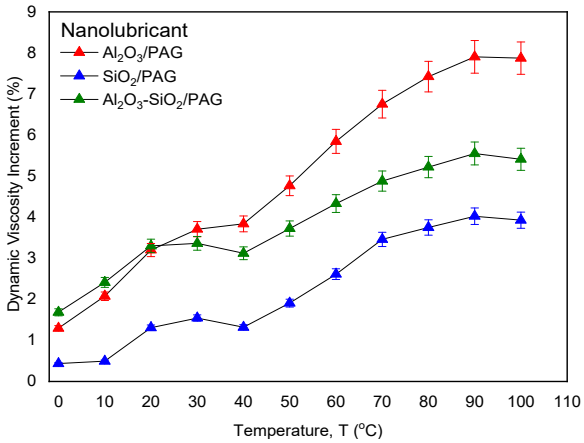

(**c**) 0.05% volume concentration

Figure 5. Dynamic viscosity increment of Al_2O_3/PAG, SiO_2/PAG and Al_2O_3-SiO_2/PAG nanolubricants at different volume concentrations.

Interestingly, the average increment of viscosity for Al_2O_3-SiO_2/DEC PAG hybrid nanolubricants was 2.74% higher than DEC PAG lubricants. As was previously observed, the viscosity of the Al_2O_3/DEC PAG and SiO_2/DEC PAG nanolubricants increased. In this instance, it was discovered that hybrid nanolubricants are at the center of this trend. This finding is due to using an 80:20 composition ratio of Al_2O_3 and SiO_2 nanoparticles to prepare Al_2O_3-SiO_2/DEC PAG hybrid nanolubricants. As a result, the viscosity of hybrid nanolubricants did not increase too much, even at the same volume concentration. These results occurred due to the complementary qualities of the two mono-component nanoparticles [12,34]. However, no clear relationship was observed for the viscosity increments at different temperatures. The viscosity increment was generally increased with increasing temperature and applied to all nanolubricants.

Regression models were developed using the present experimental data for the dynamic viscosity of nanolubricants. The theory for the viscosity of nanofluids (in the present study referring to nanolubricants) remains a hot topic of discussion among researchers. The nanofluids do not behave like ordinary two-phase liquid mixtures. Many factors need to be considered, such as shape, size, and type of nanoparticles, and the nature of the base fluids that may affect the viscosity behavior of nanofluids [35]. For hybrid nanofluids with combinations of different nanoparticles, the composition ratio for each nanoparticle in the base fluid significantly affects the viscosity properties [32]. Therefore, to date, no single model can predict viscosity for various types of nanofluids. Figure 6 presents the comparison between the viscosity estimated by the correlation from Pak and Cho [36], Brinkman [37], and Wang et al. [38] with the experimental data from the present study. It can be seen that the estimation from Brinkman [37] and Wang et al. [38] correlations can accurately predict the viscosity of Al_2O_3/PAG nanolubricants at high temperatures. However, these correlations are overpredicted and underpredicted for the viscosity of Al_2O_3/PAG nanolubricants at low temperatures. On the other hand, the estimation from Pak and Cho [36] overpredicted the viscosity of Al_2O_3/PAG nanolubricants at all temperatures. Therefore, it is necessary to develop a regression model to estimate the dynamic viscosity of the present nanolubricants.

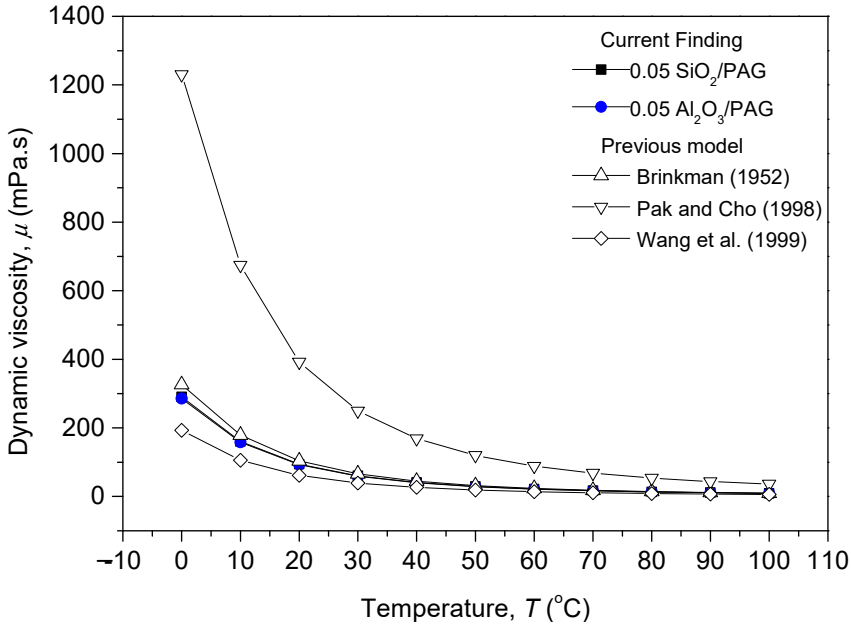

Figure 6. Comparison between experimental data and correlations from the literature [36–38].

According to the previous model, the dynamic viscosity of different nanoparticles in PAG lubricants can be expressed as a function of volume concentration and temperature [39]. The regression model in Equation (4) was developed to estimate the dynamic

viscosity of Al_2O_3/PAG, SiO_2/PAG, and Al_2O_3-SiO_2/PAG at different volume concentrations and temperatures. The constants (A and B) in dynamic viscosity Equation (4) are shown in Table 6. The constant (A and B) is generated using the least-squares method, a statistical procedure to find the best fit for a set of data points by minimizing the sum of the offsets or residuals of points from the plotted curve. The equation can predict the dynamic viscosity of Al_2O_3/PAG, SiO_2/PAG, and Al_2O_3-SiO_2/PAG nanolubricants at volume concentrations of $0 \leq \phi \leq 0.1\%$ and $0 \leq T \leq 100$ °C. The comparison between the experimental data and the estimated value of dynamic viscosity from Equation (4) is presented in Figure 7. From the figure, the equation can predict the dynamic viscosity of the present nanolubricants within ±2% difference from the experimental findings.

$$\mu_r = \frac{\mu_{NL}}{\mu_{BL}} = \left(1 + \frac{\phi}{100}\right)^A \left(1 + \frac{T}{80}\right)^B \quad (4)$$

Table 6. Dynamic viscosity correlation model's coefficient.

Nanolubricants	A	B	Average Deviation (%)	Standard Deviation (%)
Al_2O_3	77.00	0.0250	0.89	0.67
SiO_2	28.25	0.0200	0.73	0.49
Al_2O_3-SiO_2/PAG	61.07	0.0175	0.61	0.44

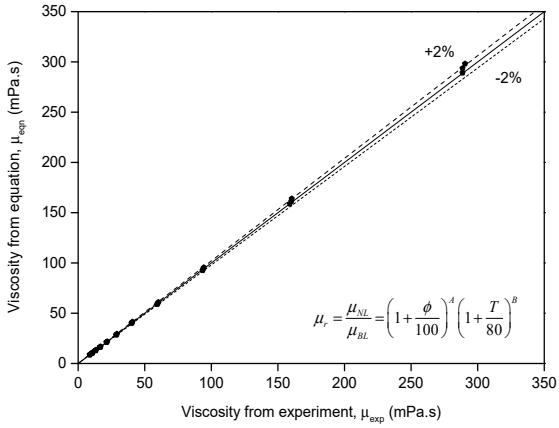

(**a**) Al_2O_3/PAG nanolubricants

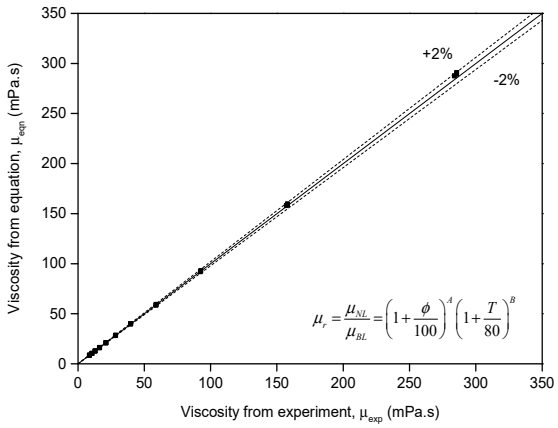

(**b**) SiO_2/PAG nanolubricants

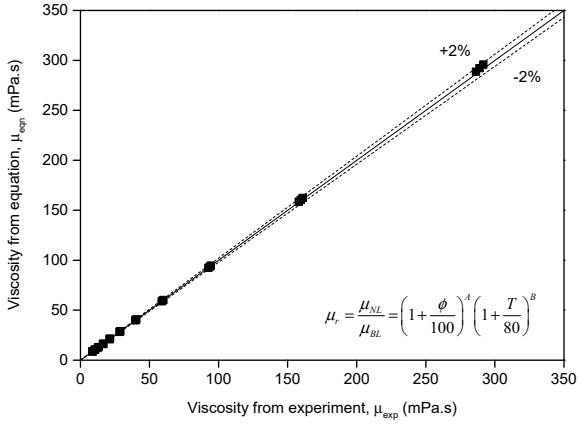

(**c**) Al_2O_3-SiO_2/PAG nanolubricants

Figure 7. Comparison between viscosity experimental data and regression equation for different nanolubricants.

From regression Equation (4), a suspension containing nanoparticles in a particular volume concentration, ϕ will affect its viscosity. The addition of nanoparticles into the PAG

lubricants will increase the fluid's internal resistance, which results in the thickening of the nanolubricants. The viscosity will increase by adding nanoparticles to a specific volume solution. However, high temperatures will reduce the viscosity of nanolubricants. The rise in temperature decreases the fluid's intermolecular forces, decreasing its resistance and viscosity [30]. Nonlinear equations are used in developing the present regression model because of the steady increment for viscosity with temperature and concentration according to the data from the experiment. A dimensionless unit of effective viscosity ratio, μ_r is the ratio of nanolubricants viscosity and PAG lubricants viscosity at a given temperature and concentration. The right-sided expression is divided by the maximum temperature and the maximum percentage of viscosity to maintain a dimensionless unit on the right side of the equation.

3.4. Viscosity Index Evaluation

Figure 8 shows the viscosity index for DEC PAG lubricants, Al_2O_3/DEC PAG, SiO_2/DEC PAG, and Al_2O_3-SiO_2/DEC PAG nanolubricants at different volume concentrations. In the figure, the viscosity indices for all nanolubricants were improved up to 6% higher than the original DEC PAG lubricants. The improved viscosity index suggests that nanolubricants can perform better than the original DEC PAG lubricants when operating under variable temperature conditions due to minimal viscosity changes at a given temperature. This attribute is essential for lubrication applications, especially during an operation inside an AAC compressor. The viscosity index is closely related to the viscosity. The increment in the viscosity index is due to the viscosity increase when nanoparticles are dispersed in DEC PAG lubricants. With a higher viscosity index, nanolubricants can enhance engine lubrication at any temperature, whether it is during a cold start or the compressor's maximum operating temperature. Similar results were also presented by a previous study in the literature [40]. The high viscosity index thickens the lubricants, particularly at high operating temperatures. Nanolubricants' lubricating effects can be extended to a wide range of temperatures and are helpful for AAC compressors.

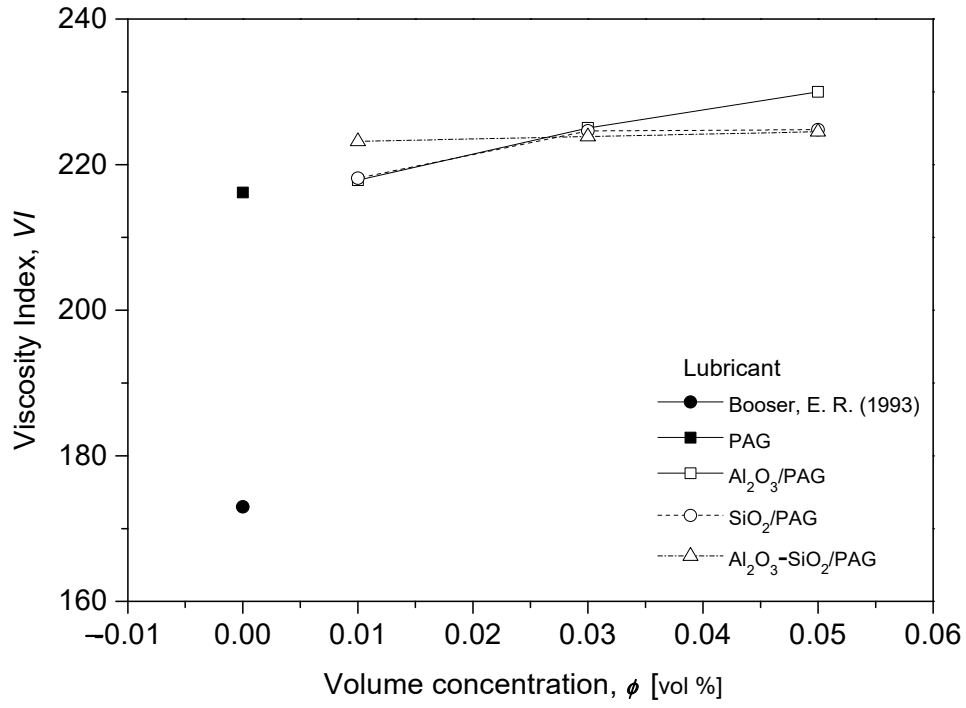

Figure 8. Viscosity index for various types of nanolubricants compared to Booser [1].

The Al_2O_3/DEC PAG nanolubricants were performed with the highest viscosity index at 0.05% volume concentration compared to SiO_2/DEC PAG and Al_2O_3-SiO_2/DEC

PAG nanolubricants. However, at a low volume concentration of 0.01%, SiO_2/DEC PAG and Al_2O_3/DEC PAG nanolubricants were recorded with a low viscosity index compared to Al_2O_3-SiO_2/DEC PAG hybrid nanolubricants. The high viscosity increments for Al_2O_3/DEC PAG nanolubricants resulted from the rise of the viscosity index, especially at high volume concentrations. Nevertheless, all types of nanolubricants recorded an almost equivalent viscosity index higher than PAG lubricants at 0.03% volume concentration. According to the manufacturer of Anton Paar viscometers, the viscosity index for glycol oil type is 200 to 220 [29]. Meanwhile, the viscosity index of nanolubricants for the present study is 217.9 to 230. This finding confirms that using nanoparticles in PAG lubricants can potentially enhance the viscosity index. High viscosity index is highly recommended for lubricants to perform with a more stable lubricating film over a wide range of operating temperatures.

3.5. Coefficient of Friction

The coefficient of friction (COF) versus sliding time for various nanolubricant concentrations is shown in Figure 9. The results show that the COF remains stable over the 1800 s of sliding time, which can be attributed to the influence of the heater that maintained the temperature of the lubricant throughout the testing. However, the running-in duration exhibits slight variations, likely due to the four balls' vigorous spinning during the friction process. Figure 9a,c reveal that the COF starts to decline only when the volume concentration of the nanolubricant reaches 0.03% compared to DEC PAG. Conversely, Figure 9b shows that the SiO_2/DEC PAG nanolubricant results in a decrease in COF at volume concentrations of 0.01% and 0.03% but an increase in COF at 0.05% compared to DEC PAG. These results indicate that using nanoparticles can reduce COF, but only at specific concentrations. For example, the average volume concentration of 0.01% decreases COF by 3.6% and 8.1% for Al_2O_3/DEC PAG and Al_2O_3-SiO_2/DEC PAG nanolubricants, respectively. The decrease in COF in nanolubricants is generally attributed to nano-sliding, which enhances the sliding contact between two surfaces [41]. The slight increase in COF observed at high concentrations of 0.05% is considered negligible, given that the COF of the base lubricant is already low. This increase in COF can be explained by the increase in viscosity, which raises the shear force of the liquid and increases the effort required to move the sliding surfaces. In the future, more research is needed to gain a deeper understanding of this behavior, particularly about nanolubricants.

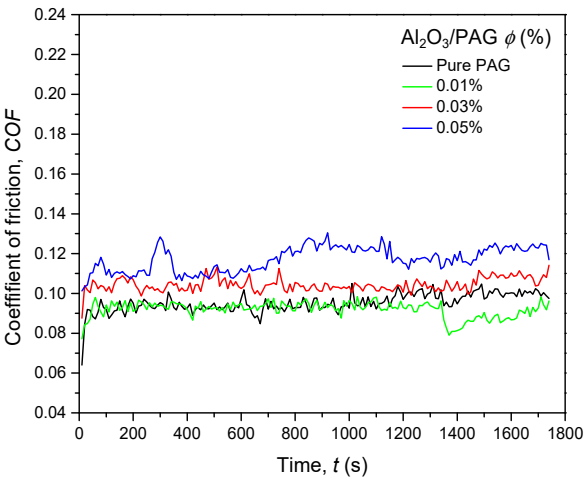

(**a**) Al_2O_3/PAG

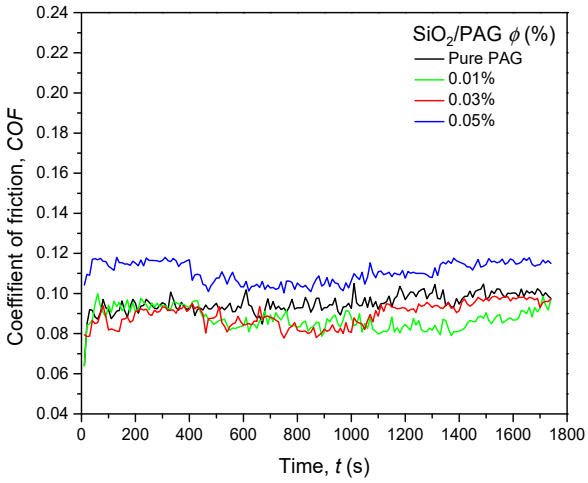

(**b**) SiO_2/PAG

Figure 9. *Cont.*

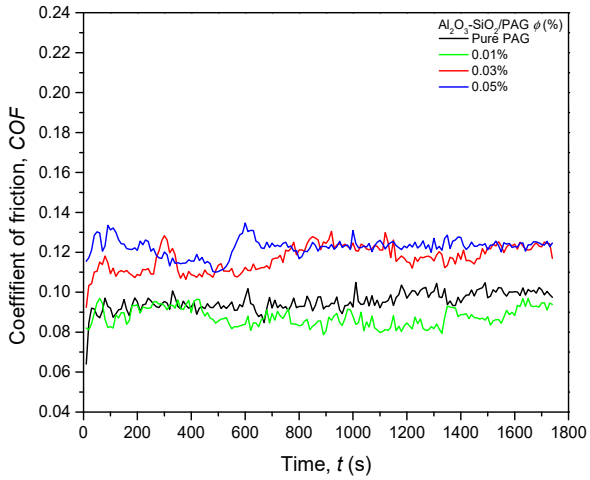

(**c**) Al_2O_3-SiO_2/PAG

Figure 9. Coefficient of friction of nanolubricants at different volume concentrations.

4. Conclusions

The studies of the effects of nanoparticles on the shear flow curve, viscosity, and coefficient of friction of the Al_2O_3/DEC PAG, SiO_2/DEC PAG, and Al_2O_3-SiO_2/DEC PAG have been summarized comprehensively in this paper. The following remarks can be extracted from the present review.

I. The rheological studies showed that the nanolubricants in the present study retain Newtonian behavior similar to the original lubricants.
II. The dynamic viscosity of all nanolubricants increases, although the viscosity increment is minimal. The SiO_2/DEC PAG has the lowest increment of velocity (1.88%), followed by Al_2O_3-SiO_2/DEC PAG and Al_2O_3-SiO_2/DEC PAG (2.74% and 3.56%).
III. The viscosity index of all nanolubricants was better only at higher concentrations.
IV. The nanoparticle additives can improve the coefficient of friction of DEC PAG lubricant. However, additional studies need to be conducted to study rheology in depth and factor in the enhancement mechanism in the tribology of the nanolubricant.

Author Contributions: Conceptualization, M.Z.S., N.N.M.Z. and W.H.A.; methodology, M.Z.S. and W.H.A.; software, M.Z.S., M.F.G. and H.M.A.; validation, M.Z.S. and N.N.M.Z.; formal analysis, M.Z.S.; investigation, M.Z.S.; resources, W.H.A., M.F.G. and H.M.A.; data curation, M.Z.S. and W.H.A.; writing—original draft preparation, M.Z.S.; writing—review and editing, M.Z.S. and N.N.M.Z.; visualization, W.H.A.; supervision, W.H.A.; project administration, W.H.A.; funding acquisition, W.H.A., M.F.G. and H.M.A. All authors have read and agreed to the published version of the manuscript.

Funding: This research was funded by Universiti Malaysia Pahang, under Distinguished Research Grant RDU223021.

Institutional Review Board Statement: Not applicable.

Informed Consent Statement: Not applicable.

Data Availability Statement: Not applicable.

Acknowledgments: The authors are grateful to Universiti Malaysia Pahang for the financial support. The authors would like to also thank the research teams from the Centre for Research in Advanced Fluid and Processes (Pusat Bendalir), Advanced Automotive Liquids Laboratory (AALL), and Interdisciplinary Research Center for Renewable Energy and Power Systems (IRC-REPS) who have provided professional insights and expertise that greatly assisted the present research work.

Conflicts of Interest: The authors declare no conflict of interest.

References

1. Booser, E.R. *CRC Handbook of Lubrication and Tribology, Volume III: Monitoring, Materials, Synthetic Lubricants, and Applications*; CRC Press: Boca Raton, FL, USA, 1993; Volume 3.
2. Azmi, W.H.; Sharif, M.Z.; Yusof, T.M.; Mamat, R.; Redhwan, A.A.M. Potential of nanorefrigerant and nanolubricant on energy saving in refrigeration system—A review. *Renew. Sustain. Energy Rev.* **2017**, *69*, 415–428. [CrossRef]
3. Hodnebrog, Ø.; Etminan, M.; Fuglestvedt, J.S.; Marston, G.; Myhre, G.; Nielsen, C.J.; Shine, K.P.; Wallington, T.J. Global warming potentials and radiative efficiencies of halocarbons and related compounds: A comprehensive review. *Rev. Geophys.* **2013**, *51*, 300–378. [CrossRef]
4. Wang, C.C. System performance of R-1234yf refrigerant in air-conditioning and heat pump system—An overview of current status. *Appl. Therm. Eng.* **2014**, *73*, 1412–1420. [CrossRef]
5. Sharif, M.Z.; Azmi, W.H.; Zawawi, N.N.M.; Ghazali, M.F. Comparative air conditioning performance using SiO_2 and Al_2O_3 nanolubricants operating with Hydrofluoroolefin-1234yf refrigerant. *Appl. Therm. Eng.* **2022**, *205*, 118053. [CrossRef]
6. Sharif, M.Z.; Azmi, W.H.; Mamat, R.; Shaiful, A.I.M. Mechanism for improvement in refrigeration system performance by using nanorefrigerants and nanolubricants—A review. *Int. Commun. Heat Mass Transf.* **2018**, *92*, 56–63. [CrossRef]
7. Zawawi, N.N.M.; Azmi, W.H.; Ghazali, M.F. Tribological performance of Al2O3–SiO2/PAG composite nanolubricants for application in air-conditioning compressor. *Wear* **2022**, *492–493*, 204238. [CrossRef]
8. Ma, J.; Shahsavar, A.; Al-Rashed, A.A.A.A.; Karimipour, A.; Yarmand, H.; Rostami, S. Viscosity, cloud point, freezing point and flash point of zinc oxide/SAE50 nanolubricant. *J. Mol. Liq.* **2020**, *298*, 112045. [CrossRef]
9. Haldar, A.; Chatterjee, S.; Kotia, A.; Kumar, N.; Ghosh, S.K. Analysis of rheological properties of MWCNT/SiO_2 hydraulic oil nanolubricants using regression and artificial neural network. *Int. Commun. Heat Mass Transf.* **2020**, *116*, 104723. [CrossRef]
10. Kedzierski, M.A.; Brignoli, R.; Quine, K.T.; Brown, J.S. Viscosity, density, and thermal conductivity of aluminum oxide and zinc oxide nanolubricants. *Int. J. Refrig.* **2017**, *74*, 3–11. [CrossRef] [PubMed]
11. Zawawi, N.N.M.; Azmi, W.H.; Sharif, M.Z.; Najafi, G. Experimental investigation on stability and thermo-physical properties of Al_2O_3–SiO_2/PAG nanolubricants with different nanoparticle ratios. *J. Therm. Anal. Calorim.* **2019**, *135*, 1243–1255. [CrossRef]
12. Zawawi, N.N.M.; Azmi, W.H.; Redhwan, A.A.M.; Sharif, M.Z.; Samykano, M. Experimental investigation on thermo-physical properties of metal oxide composite nanolubricants. *Int. J. Refrig.* **2018**, *89*, 11–21. [CrossRef]
13. Aliasgari, M.; Maleki-Jirsaraei, N.; Rouhani, S. The effect of liquid viscosity on sliding friction coefficient of wet granular materials. In Proceedings of the EPJ Web of Conferences, Buenos Aires, Argentina, 6 August 2021; p. 08003.
14. Fatehallah, H.S.; Hammoudi, Z.S.; Zidane, L.Y. Study the effect of oil viscosity on friction coefficient at point contact elasto-hydrodynamic lubrication based on experimental analysis. *Diyala J. Eng. Sci.* **2020**, *13*, 17–21. [CrossRef]
15. Bhanvase, B.; Barai, D. *Nanofluids for Heat and Mass Transfer: Fundamentals, Sustainable Manufacturing and Applications*; Academic Press: Cambridge, MA, USA, 2021.
16. Paul, G.; Hirani, H.; Kuila, T.; Murmu, N. Nanolubricants dispersed with graphene and its derivatives: An assessment and review of the tribological performance. *Nanoscale* **2019**, *11*, 3458–3483. [CrossRef]
17. Gara, L.; Zou, Q. Friction and wear characteristics of water-based ZnO and Al_2O_3 nanofluids. *Tribol. Trans.* **2012**, *55*, 345–350. [CrossRef]
18. Jeng, Y.-R.; Huang, Y.H.; Tsai, P.C.; Hwang, G.L. Tribological properties of carbon nanocapsule particles as lubricant additive. *J. Tribol.* **2014**, *136*, 041801. [CrossRef]
19. Jeng, Y.R.; Huang, Y.H.; Tsai, P.C.; Hwang, G.L. Tribological performance of oil-based lubricants with carbon-Fe nanocapsules additive. *Tribol. Trans.* **2015**, *58*, 924–929. [CrossRef]
20. Rapoport, L.; Bilik, Y.; Feldman, Y.; Homyonfer, M.; Cohen, S.R.; Tenne, R. Hollow nanoparticles of WS_2 as potential solid-state lubricants. *Nature* **1997**, *387*, 791–793. [CrossRef]
21. Karimipour, A.; Malekahmadi, O.; Karimipour, A.; Shahgholi, M.; Li, Z. Thermal conductivity enhancement via synthesis produces a new hybrid mixture composed of copper oxide and multi-walled carbon nanotube dispersed in water: Experimental characterization and artificial neural network modeling. *Int. J. Thermophys.* **2020**, *41*, 116. [CrossRef]
22. Beijing-Deke-Daojin. Nano Silica. Available online: http://dknano.com/Ecplb.asp?Fid=1177&ClassId=1190&NewsId=2993 (accessed on 25 January 2023).
23. Sigma-Aldrich. Aluminum Oxide (13 nm) Produced by Sigma Aldrich. Available online: https://www.sigmaaldrich.com/MY/en/product/aldrich/718475 (accessed on 19 December 2022).
24. Idemitsu-Kosan. Idemitsu Hermetic Oil 1234yf ND12. Available online: https://www.idemitsulubricants.com/product/idemitsu-hermetic-oil-1234yf (accessed on 5 January 2023).
25. Nayerdinzadeh, S.; Babadi Soultanzadeh, M.; Haratian, M.; Zamanimehr, A. Experimental and numerical evaluation of thermal performance of parabolic solar collector using water/Al_2O_3 nano-fluid: A case study. *Int. J. Thermophys.* **2020**, *41*, 1–21. [CrossRef]
26. Nugroho, A.; Bo, Z.; Mamat, R.; Azmi, W.H.; Najafi, G.; Khoirunnisa, F. Extensive examination of sonication duration impact on stability of Al_2O_3-Polyol ester nanolubricant. *Int. Commun. Heat Mass Transf.* **2021**, *126*, 105418. [CrossRef]
27. Schulz, E.F.; Wilde, R.H.; Albertson, M.L. Influence of Shape on the Fall Velocity of Sedimentary Particles. Doctoral Dissertation, Colorado State University, Fort Collins, CO, USA, 1954.
28. Ghadimi, A.; Saidur, R.; Metselaar, H.S.C. A review of nanofluid stability properties and characterization in stationary conditions. *Int. J. Heat Mass Transf.* **2011**, *54*, 4051–4068. [CrossRef]

29. RheolabQC, A.P. Viscometer ISO 17025 Calibration. Available online: https://www.anton-paar.com/my-en/services-support/iso-17025-calibration/ (accessed on 25 January 2023).
30. Rao, Y. Nanofluids: Stability, phase diagram, rheology and applications. *Particuology* **2010**, *8*, 549–555. [CrossRef]
31. Asadi, M.; Asadi, A. Dynamic viscosity of MWCNT/ZnO–engine oil hybrid nanofluid: An experimental investigation and new correlation in different temperatures and solid concentrations. *Int. Commun. Heat Mass Transf.* **2016**, *76*, 41–45. [CrossRef]
32. Hamid, K.A.; Azmi, W.H.; Nabil, M.F.; Mamat, R.; Sharma, K.V. Experimental investigation of thermal conductivity and dynamic viscosity on nanoparticle mixture ratios of TiO_2-SiO_2 nanofluids. *Int. J. Heat Mass Transf.* **2018**, *116*, 1143–1152. [CrossRef]
33. Nugroho, A.; Mamat, R.; Bo, Z.; Azmi, W.H.; Alenezi, R.; Najafi, G. An overview of vapor compression refrigeration system performance enhancement mechanism by utilizing nanolubricants. *J. Therm. Anal. Calorim.* **2022**, *147*, 9139–9161. [CrossRef]
34. Sundar, L.S.; Irurueta, G.O.; Ramana, E.V.; Singh, M.K.; Sousa, A.C.M. Thermal conductivity and viscosity of hybrid nanfluids prepared with magnetic nanodiamond-cobalt oxide (ND-Co_3O_4) nanocomposite. *Case Stud. Therm. Eng.* **2016**, *7*, 66–77. [CrossRef]
35. Azmi, W.H.; Sharma, K.V.; Mamat, R.; Najafi, G.; Mohamad, M.S. The enhancement of effective thermal conductivity and effective dynamic viscosity of nanofluids—A review. *Renew. Sustain. Energy Rev.* **2016**, *53*, 1046–1058. [CrossRef]
36. Pak, B.C.; Cho, Y.I. Hydrodynamic and heat transfer study of dispersed fluids with submicron metallic oxide particles. *Exp. Heat Transf. Int. J.* **1998**, *11*, 151–170. [CrossRef]
37. Brinkman, H.C. The viscosity of concentrated suspensions and solutions. *J. Chem. Phys.* **1952**, *20*, 571. [CrossRef]
38. Wang, X.; Xu, X.; Choi, S.U.-S. Thermal conductivity of nanoparticle-fluid mixture. *J. Thermophys. Heat Transf.* **1999**, *13*, 474–480. [CrossRef]
39. Sharma, K.V.; Sarma, P.K.; Azmi, W.H.; Mamat, R.; Kadirgama, K. Correlations to predict friction and forced convection heat transfer coefficients of water based nanofluids for turbulent flow in a tube. *Int. J. Microscale Nanoscale Therm. Fluid Transp. Phenom.* **2012**, *3*, 1–25.
40. Hemmat Esfe, M.; Abbasian Arani, A.A.; Esfandeh, S. Improving engine oil lubrication in light-duty vehicles by using of dispersing MWCNT and ZnO nanoparticles in 5W50 as viscosity index improvers (VII). *Appl. Therm. Eng.* **2018**, *143*, 493–506. [CrossRef]
41. Man, W.; Huang, Y.; Gou, H.; Li, Y.; Zhao, J.; Shi, Y. Synthesis of novel CuO@Graphene nanocomposites for lubrication application via a convenient and economical method. *Wear* **2022**, *498–499*, 204323. [CrossRef]